Far-from-equilibrium Ostwald ripening in electrostatically driven granular powders

M.V. Sapozhnikov[1,2], A. Peleg[3], B. Meerson[4], I.S. Aranson[1], and K.L. Kohlstedt[5]
[1] *Argonne National Laboratory, 9700 S. Cass Avenue, Argonne, IL 60439*
[2] *Institute for Physics of Microstructures, Russian Academy of Sciences, GSP-105, Nizhny Novgorod 603600, Russia*
[3] *Theoretical Division, Los Alamos National Laboratory, Los Alamos, NM 87545*
[4] *Racah Institute of Physics, Hebrew University of Jerusalem, Jerusalem 91904, Israel and*
[5] *Department of Physics and Astronomy, University of Kansas, Lawrence, KS 66045*

We report the first experimental study of cluster size distributions in electrostatically driven granular submonolayers. The cluster size distribution in this far-from-equilibrium process exhibits dynamic scaling behavior characteristic of the (nearly equilibrium) Ostwald ripening, controlled by the attachment and detachment of the "gas" particles. The scaled size distribution, however, is different from the classical Wagner distribution obtained in the limit of a vanishingly small area fraction of the clusters. A much better agreement is found with the theory of Conti *et al.* [Phys. Rev. E **65**, 046117 (2002)] which accounts for the cluster merger.

PACS numbers: 45.70.Mg, 45.70.Qj

Dynamics of big assemblies of macroscopic particles are poorly understood, especially when inter-particle interactions are strongly dissipative [1, 2]. Additional complications arise when the grain size goes below 0.1 mm, and non-trivial contact interactions come into play. As small particles acquire an electric charge, the dynamics are governed by the interplay between long-range electrostatic and short-range contact forces. On the other hand, an efficient electrostatic excitation of granular media becomes possible here, and offers new opportunities for investigation and control.

Recently, a host of fascinating pattern-formation phenomena and far-from-equilibrium phase separation processes have been observed in electrostatically driven granular powders, in air or vacuum [3, 4, 5, 6] and in poorly conducting liquids [7]. One of them is cluster coarsening which is remarkably similar to the Ostwald ripening [8, 9], despite the fact that the system is very far from equilibrium. This work deals with experiment and theory of this process. We work with submonolayers of metallic powders, i.e., the layer of particles only partially covers the bottom of the experimental cell, and it is approximately one-particle high. Conducting particles (we used $40\,\mu m$ spherical copper particles, the total number of particles was about 10^7) are placed between the plates of a large plane capacitor, levelled horizontally. We used 27×27 cm transparent capacitor plates (glass coated by indium doped tin oxide); the plate spacing was $1.5\,mm$. The DC electric field E in the capacitor was varied in the range $0 - 7\,kV/cm$. The experiments were performed in the atmosphere of dry nitrogen to reduce adhesion of particles on the plate due to humidity of air. Visualization was achieved with a CCD camera mounted above the cell.

When particles are in contact with the capacitor plate, they acquire an electric charge. If the electric field in the cell E exceeds a critical value, the resulting upward electric force overcomes the particle weight and pushes the particles upward. When a particle hits the upper plate, it recharges and falls back. Remarkably, the collective behavior of this far-from-equilibrium system closely resembles that of phase separating systems close to equilibrium [3, 4, 5, 6]. The role of temperature, however, is played by the electric field E. The particles remain immobile on the bottom plate of the capacitor, and form a precipitate phase, at $E < E_1$. If the field E is larger than a second threshold value, $E_2 > E_1$, the particles form a gas-like phase. This second field E_2 is 50%-70% larger than E_1. Upon "quenching" the field into the coexistence region $E_1 < E < E_2$ one observes nucleation of precipitate, and small densely packed clusters form and start to grow on the bottom plate. Then the clusters undergo coarsening: larger clusters grow at the expense of smaller ones (which shrink and disappear). This far-from-equilibrium coarsening process closely resembles the Ostwald ripening with *attachment-detachment* (in a different terminology *interface-controlled*) kinetics [9].

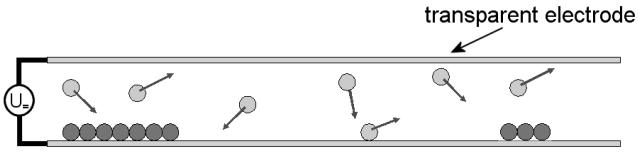

FIG. 1: A schematic of experimental setup.

The basic physics behind phase separation and coarsening in this system was investigated previously [3, 5, 6]. Two main physical processes are at work here. On the one hand, there is electrostatic screening: a decrease in the vertical electric force F, exerted on a grain in contact with the bottom plate, caused by the presence of other grains. On the other hand, collisions between the grains and the bottom plate, and between the grains themselves, are strongly inelastic, so the granular temperature is of no importance. The reader is referred to Refs. [3, 5] for

detail, including quantitative estimates of the respective forces *etc.*

At the coarsening stage the clusters compete for the material, and this competition is mediated by the gas phase. A preliminary scaling analysis of experimental data on the cluster coarsening dynamics [3] and special measurements of the shrinkage rate of single clusters [6] strongly indicated that the cluster growth/coarsening is limited by the attachment-detachment rates of the "gas" particles, rather than by the transport rate in the "gas" phase. Correspondingly, a phenomenological continuum model of this phase separation and coarsening was formulated in Ref. [5] in terms of a Ginzburg-Landau equation subject to conservation of the total number of grains. Similar globally-conserved Ginzburg-Landau equations have been studied in different contexts [10, 11, 12]. In the regime of well-developed (densely-packed) clusters the continuum model yields "sharp-interface" equations which govern the dynamics of the inter-phase boundary and are very useful in the analysis of the late-time stage of the phase separation [5].

This work focuses on the statistical dynamics of this far-from-equilibrium Ostwald ripening process. One advantage of our new experimental apparatus is a very large aspect ratio, allowing us, for the first time, to produce a large number of clusters and accumulate sufficient statistics. By following the dynamic scaling properties of the cluster size distribution we establish with confidence the attachment-detachment character of kinetics. Surprisingly, the scaled size distribution of the clusters turns out to be quite different from the classical Wagner distribution [9]. A much better agreement with experiment is found when we employ a more advanced theory by Conti *et al.* [12] which, in addition to the cluster growth/shrinking processes, accounts for the cluster merger. The theory has no adjustable parameters and is very different, both in its assumptions and predictions, from a recent phenomenological exchange-driven growth model suggested by Ben-Naim and Krapivsky [13].

Figure 2 shows a typical sequence of snapshots of the system in the coexistence region $E_1 < E < E_2$. The Ostwald ripening process is clearly seen. In addition, distinct merger events are observed. Figure 3a shows the average cluster area $\langle A\rangle(t)$ versus time. This dependence is very close to linear. Introducing the cluster radius $R = (A/\pi)^{1/2}$, we find that the mean-square radius $R_*(t) \equiv \langle R^2\rangle^{1/2}$ grows with time like $t^{1/2}$. This is a defining feature of the attachment-detachment-controlled Ostwald ripening [9]. The plot of the inverse number of clusters in the cell N^{-1} versus time (Fig. 3b) approaches a straight line which implies a scaling behavior $N(t) \sim t^{-1}$. An additional support for the scaling is provided by the approximate constancy of the total area of the clusters at late time, $N(t)\, R_*(t)^2 \sim const$, see Fig. 4. The dynamic range of Figs. 3 and 4 is limited by 5.40×10^4, since for later times the number of clusters is too small.

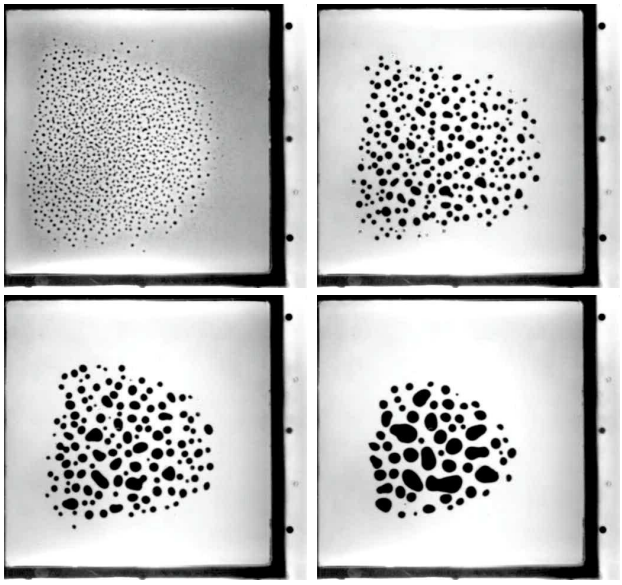

FIG. 2: Snapshots of coarsening of granular clusters in electrostatic cell at times (in seconds) $t = 0$ (upper left), 1×10^4 (upper right), 2×10^4 (lower left) and 5×10^4 sec (lower right). The applied DC electric field $E = 2.33$ kV/cm.

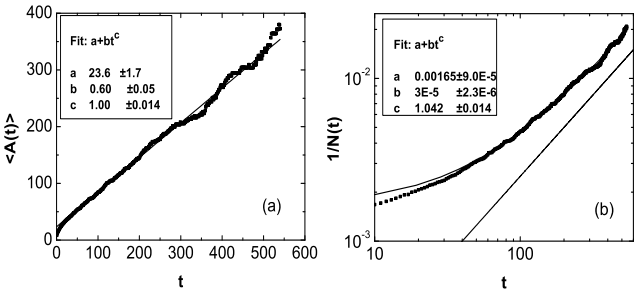

FIG. 3: The average cluster area $\langle A\rangle$ (a) and the inverse number of clusters in the cell $1/N$ (b) versus time in the experiment shown in Fig. 2. The unit of time in this figure corresponds to 100 *sec*. The solid curves (see also the insets) show data fits of the type $a + b\, t^c$. The straight line in figure b, shown for reference, has slope 1. Notice that in the experiments we waited for about two minutes (until small clusters nucleated at the bottom plate) before starting the measurements. As a result, the $\langle A\rangle(t)$ curve does not pass through the origin.

A more detailed characterization of the far-from-equilibrium Ostwald ripening is provided by the dynamics of the probability distribution function (PDF) of the cluster sizes $f(R,t)$. The PDF is defined as usual:

$$\int_0^\infty f(R,t)\, dR = N(t)/L^2\,, \qquad (1)$$

where L^2 is the cell area. Dynamic scaling behavior of $f(R,t)$ is expected at late times, when the total area of

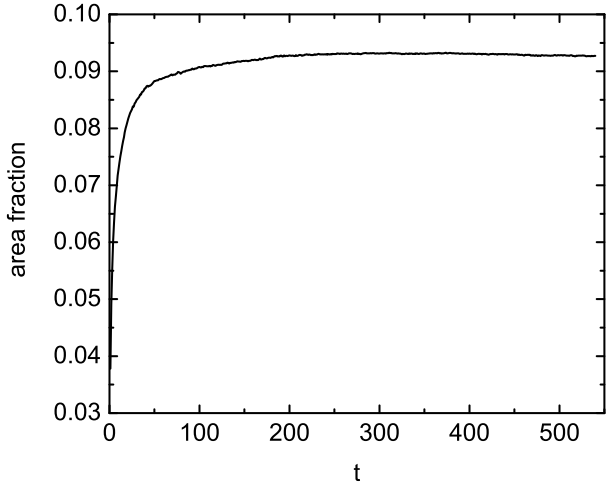

FIG. 4: The area fraction of the clusters (the total area of the clusters divided by the area of the cell) versus time. The unit of time corresponds to 100 *sec*. The dynamic scaling regime is observed at late times, when the area fraction approaches a constant value.

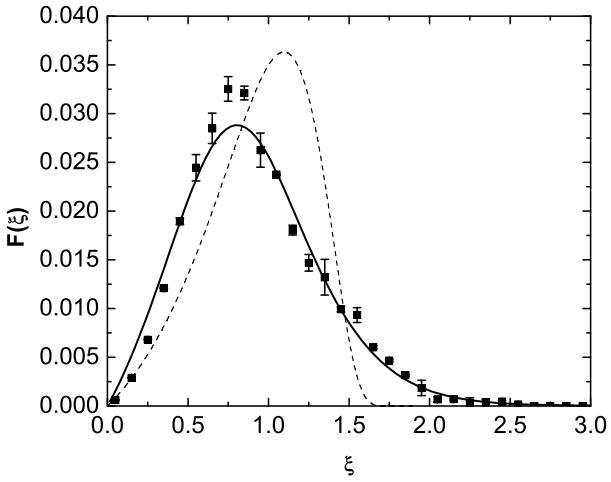

FIG. 5: Scaled probability distribution function (PDF) of cluster sizes $F(\xi)$, where $\xi = R/R_*(t)$ [see Eq. (3)]. The squares show the experimental results, obtained from 340 snapshots from the interval $2.01 \times 10^4\,\mathrm{sec} \le t \le 5.40 \times 10^4$ sec and averaged over 4 experiments. The error bars are not shown when they are smaller than the size of the square. The dotted line is the Wagner distribution $F_W(\xi)$ [see Eq. (8)], for the same area fraction $\varepsilon = 0.092$ as in the experiment. The solid line shows the scaled PDF, obtained from the theory of the attachment-detachment-controlled Ostwald ripening with coalescence [12] for the same area fraction.

the clusters approaches a constant:

$$\pi \int_0^\infty f(R,t)\, R^2 dR = \varepsilon\,. \tag{2}$$

Here ε is the area fraction of the clusters: the ratio of the total area of all clusters to the cell area L^2. In view of Eq. (2), the expected scaling behavior is

$$f(R,t) = R_*^{-3}(t)\, F\left[R/R_*(t)\right]\,. \tag{3}$$

Using the Ansatz (3), we can express the number of clusters (1) and the mean squared radius $R_*^2(t)$ through the moments of the scaled PDF $F(\xi)$:

$$\frac{N(t)}{L^2} = \frac{m_0}{R_*^2(t)}\,, \tag{4}$$

$$R_*^2(t) \equiv \langle R^2\rangle = \frac{\int_0^\infty f(R,t) R^2\, dR}{\int_0^\infty f(R,t)\, dR} = \frac{m_2}{m_0}\, R_*^2(t)\,, \tag{5}$$

where $m_k = \int_0^\infty F(\xi)\, \xi^k d\xi$, $k = 0, 1, \ldots$. Equation (5) yields a consistency condition $m_2 = m_0$.

The imaging processing and tracking of the cluster growth and coarsening in our experiment was performed using the MATLAB 6 toolbox. The scaled PDF, obtained by averaging over 4 different experiments, performed under the same conditions, is shown in Fig. 5. The horizontal axis shows the cluster radius divided by $R_*(t)$, the vertical axis shows the experimental PDFs multiplied by $R_*^3(t)$. The scaled PDF is the result of collapse of 340 original, unscaled PDFs from the 4 experiments, measured in the time range $2.01 \times 10^4\,\mathrm{sec} \le t \le 5.40 \times 10^4$ sec with equal 100 sec time intervals. We checked that the late-time values of the cluster area fractions in these 4 experiments were close to each other: 9.1%, 9.3% (in two experiments) and 9.4%.

What is the theoretical prediction for the scaled PDF $F(\xi)$? Let us first proceed by neglecting the cluster merger. In this case the PDF dynamics is described by a continuity equation in the space of cluster sizes:

$$\partial_t f + \partial_R\left(\dot{R} f\right) = 0\,. \tag{6}$$

For the attachment-detachment-controlled kinetics, the cluster growth/shrinking law is

$$\dot{R} = D\left(\frac{1}{R_c(t)} - \frac{1}{R}\right)\,, \tag{7}$$

where $R_c(t)$ is the time-dependent *critical* radius, while the effective diffusivity D depends on the electric field E and on the size and weight of the grains [5]. The growth law (7) is obtained under assumption that the particle transport in the gas phase is very fast, so that the concentration of the gas phase in the cell is approximately uniform in space, varying only in time. The inverse critical radius $1/R_c(t)$ in Eq. (7) is proportional to the (time-dependent) difference between the concentration of the gas phase and a constant value of this concentration, for which a planar interface of the cluster phase is at rest [5]. Equation (7) describes shrinking and disappearance of small clusters, for which $R < R_c$. The shrinking occurs in a finite time. At $R \ll R_c$ the area of the shrinking cluster goes down linearly as the time

increases. This property was checked in experiment, and was found to hold until the shrinking clusters become small compared to the gap between the capacitor plates, and three-dimensional effects come into play [6].

Equations (6) and (7), together with the cluster area conservation (2), make a closed set. Mathematically, this model is identical to the Wagner's model of the attachment-detachment-controlled Ostwald ripening [9]. (The attachment-detachment-controlled systems are quite different from the *diffusion*-controlled systems, for which a theory of cluster coarsening, valid for vanishingly small area fractions of the clusters, was developed earlier by Lifshitz and Slyozov [8].) An immediate consequence of Eqs. (2), (6) and (7) is the equality

$$R_c(t) = \langle R \rangle(t) = \frac{\int_0^\infty f(R,t) R\, dR}{\int_0^\infty f(R,t)\, dR}\,.$$

For the scaling solutions (3) we obtain $R_c(t) = \langle R \rangle(t) = (m_1/m_0) R_*(t)$. Therefore, at large times $\langle R \rangle(t) = const\,(Dt)^{1/2}$ and, in view of Eq. (4), $N(t)/L^2 = const\,(Dt)^{-1}$, where the prefactors depend on ε. Employing the Ansatz (3) and solving the resulting ordinary differential equation, one arrives at a *family* of solutions for $F(\xi)$, all of which have a compact support $0 < \xi < \xi_m$. The problem of selection of the correct scaled PDF out of this family of solutions has been extensively studied [11, 14, 15, 16]. A special role here is played by the Wagner distribution,

$$F_W(\xi) = \begin{cases} \frac{C\varepsilon\,\xi}{(\xi_m - \xi)^4}\, \exp\left(-\frac{2\,\xi_m}{\xi_m - \xi}\right) & \text{if } 0 < \xi < \xi_m, \\ 0 & \text{if } \xi > \xi_m, \end{cases} \quad (8)$$

for which $\xi_m = \left[1 + 2e^2\, Ei(-2)\right]^{-1/2} \simeq 1.8989$ is the largest. Also, $C = \pi^{-1}\left[1/(2e^2) + Ei(-2)\right]^{-1} \simeq 16.961$, and $Ei\,(...)$ is the exponential integral function [17]. The Wagner distribution for $\varepsilon = 0.092$ (the same area fraction as in experiment) is shown in Fig. 5. One can see a large discrepancy between the Wagner distribution and the one observed in experiment.

The Wagner's model is inaccurate because it disregards the cluster merger. Therefore, we employed the more advanced theory of Conti *et al.* [12] which accounts, within the framework of the Ostwald ripening, for the binary coalescence of clusters (growing clusters merge upon touching each other). Now Eq. (6) gives way to the following kinetic equation:

$$\partial_t f + \partial_R\left(\dot{R} f\right) = -\frac{1}{2}\int_0^\infty \int_0^\infty \{2M(R_1,R_2) \times \left[\delta(R-R_1) + \delta(R-R_2) - \delta\left(R - \sqrt{R_1^2 + R_2^2}\,\right)\right] \times f(R_1,t)\, f(R_2,t)\, dR_1\, dR_2\}\,, \quad (9)$$

where $M(R_1,R_2) = \pi\,(R_1+R_2)\,(\dot{R}_1+\dot{R}_2)\,\theta(\dot{R}_1+\dot{R}_2)$, $\theta(\dots)$ is the step function, and $\dot{R}_1$ and $\dot{R}_2$ are governed by the same growth law (7). We refer the reader to Ref. [12] for a derivation of Eq. (9). Remarkably, Eqs. (2), (7) and (9) admit the same scaling Ansatz (3). The scaled PDF is described by a nonlinear integro-differential equation [which follows from Eq. (9)], subject to $m_2 = m_0 = \varepsilon/\pi$. The integro-differential equation can be reduced to an integral equation and solved iteratively [12]. A crucial role in the iteration procedure is played by the (non-normalizable) solutions of the Wagner problem which have an infinite support $0 < \xi < \infty$. The solution of the problem is unique (and normalizable), so the account of merger resolves the selection problem intrinsic to the Wagner's formulation. Figure 5 shows the scaled PDF, obtained by the iteration procedure [12] for the same area fraction $\varepsilon = 0.092$ as in the experiment. One can see that the agreement is much better than for the Wagner distribution. Importantly, the only parameter which enters the theory of the scaled PDF is the area fraction ε. Therefore, for a given area fraction, a comparison of the theory and experiment does not involve *any* adjustable parameters. As can be seen from Fig. 5, the theory works very well in describing the position of the maximum of the scaled PDF and the shape of the PDF to the right of the maximum, including the tail. On the other hand, the theory overestimates the number of clusters at very small scaled radii and underestimates it in the region of the maximum of the PDF. This relatively small but systematic disagreement may result from the assumption of an infinitely fast transport in the gas phase. If this assumption is relaxed, inter-cluster correlations will appear which should reduce the effective merger rate. In our experiment, however, this reduction is mitigated by the fact that, as time elapses, more material gets concentrated in the middle of the cell (see Fig. 2). The future work should attempt to account for these two competing effects.

In summary, we investigated the statistical dynamics of clusters in electrostatically-driven granular powders. We found that a recent advanced theory of the attachment-detachment-controlled Ostwald ripening [12] yields a good quantitative description of this *far-from-equilibrium* system. It is tempting to also apply this kind of analysis to mechanically vibrated granular monolayers which exhibit strikingly similar non-equilibrium phase separation properties [6, 18].

We thank J.S. Olafsen and P.V. Sasorov for useful discussions. This research was supported by the US DOE, Office of Basic Energy Sciences (grant # W-31-109-ENG-38) and by the Israel Science Foundation (grant No. 180/02).

[1] H.M. Jaeger, S.R. Nagel, and R.P. Behringer, Rev. Mod. Phys. **68**, 1259 (1996); Physics Today **49** (4), 32 (1996).
[2] L.P. Kadanoff, Rev. Mod. Phys. **71**, 435 (1999).

[3] I.S. Aranson, D. Blair, V.A. Kalatsky, G.W. Crabtree, W.K. Kwok, V.M. Vinokur, and U. Welp, Phys. Rev. Lett. **84**, 3306 (2000).
[4] D.W. Howell, I.S. Aranson, and G.W. Crabtree, Phys. Rev. E **63**, 050301(R) (2001).
[5] I.S. Aranson, B. Meerson, P.V. Sasorov, and V.M. Vinokur, Phys. Rev. Lett. **88**, 204301 (2002).
[6] M.V. Sapozhnikov, I.S. Aranson, and J.S. Olafsen, Phys. Rev. E **67** 010302(R) (2003).
[7] M.V. Sapozhnikov, Y.V. Tolmachev, I.S. Aranson, and W.K. Kwok, Phys. Rev. Lett. **90**, 114301 (2003).
[8] I.M. Lifshitz and V.V. Slyozov, Zh. Eksp. Teor. Fiz. **35**, 479 (1958) [Sov. Phys. JETP **8**, 331 (1959)]; J. Phys. Chem. Solids, **19**, 35 (1961).
[9] C. Wagner, Z. Elektrochem. **65**, 681 (1961).
[10] L. Schimansky-Geier, C. Zülicke and E. Schöll, Z. Phys. B-Cond. Mat. **84**, 433 (1991); J. Rubinstein and P. Sternberg, IMA J. Appl. Math. **48**, 249 (1992); C. Sire and S.N. Majumdar, Phys. Rev. Lett. **74**, 4321 (1995); A.D. Rutenberg, Phys. Rev. E **54**, 972 (1996); B. Meerson and I. Mitkov, Phys. Rev. E **54**, 4644 (1996); A. Peleg, M. Conti, and B. Meerson, Phys. Rev. E **64**, 036127 (2001).
[11] B. Meerson and P.V. Sasorov, Phys. Rev. E **53**, 3491 (1996).
[12] M. Conti, B. Meerson, A. Peleg, and P.V. Sasorov, Phys. Rev. E **65**, 046117 (2002).
[13] E. Ben-Naim and P. L. Krapivsky, Phys. Rev. E **68**, 031104 (2003).
[14] I. Aranson, B. Meerson and P.V. Sasorov, Phys. Rev. E **52**, 948 (1995).
[15] B. Giron, B. Meerson and P.V. Sasorov, Phys. Rev. E **58**, 4213 (1998).
[16] B. Meerson, Phys. Rev. E **60**, 3072 (1999).
[17] M. Abramowitz and I.A. Stegun, *Handbook of Mathematical Functions* (National Bureau of Standards, Washington, D.C., 1968), Chapter 5.
[18] J.S. Olafsen and J.S. Urbach, Phys. Rev. Lett. **81**, 4369 (1998).